Pramāṇa, Vol. 23, No. 3, September 1984, pp. 279–295. © Printed in India.

Raman effect in the x-ray region

ASHOK PIMPALE and CHINTAMANI MANDE*
Department of Physics, University of Poona, Pune 411 007, India
*Department of Physics, Nagpur University, Nagpur 440 010, India

Abstract. This paper presents a brief review of x-ray Raman scattering and some of our calculations on Raman scattered line shapes from light elements. We summarise the history of the Raman process in the x-ray region and present a detailed theory of the Raman scattering from an atomic many-electron system. Actual calculations of the Raman cross-section using this theory in single-particle approximation are given. The process of internal resonance Raman scattering is also discussed in the same formulation. The Raman cross-section is compared with the cross-sections of other x-ray scattering processes.

Keywords. Raman scattering; x-ray spectroscopy; internal resonance; matrix element; single particle approximation; Raman cross-section.

1. Introduction

The study of interaction between radiation and matter has provided considerable insight in understanding the physical phenomena during the last few decades. One such instance is that of Raman scattering which can be described as inelastic scattering of radiation involving transitions between discrete localized states of the scatterer. The Raman effect was first observed in the optical region of the electromagnetic spectrum and Professor C V Raman won international acclaim for this basic discovery. The discrete states involved when one uses ultraviolet, visible or infrared radiation are the rotational and vibrational states of atoms/molecules or phonons in solids with transition energies from about an electron volt to about a few milli electron volts. By now, with the advent of laser, Raman spectroscopy has become a standard and a very important tool to study such states in various materials. The corresponding process of Raman scattering in the x-ray region ($\hbar\omega \sim$ keV) involving electronic transitions between bound states of atoms has, however, had a rather chequered development. We shall try to review in brief the work done on Raman scattering in the x-ray region, present some of our results and indicate some future possibilities of this field which we feel has not yet received the attention it deserves. In this article which has been specially prepared on the occasion of the golden jubilee of the Indian Academy of Sciences, which was founded by Professor C V Raman, we wish to pay our tributes to the great genius of India.

2. Early history of x-ray Raman scattering

Historically, it seems that Smekel (1923) was the first to point out theoretically the possibility of x-ray Raman scattering. Compton (1923), in his paper on inelastic

scattering of x-rays from bound electrons, also noted the possibility of electronic transitions to unoccupied discrete states in the act of scattering, but he concluded that the probability of such a process was negligible and that the effect was experimentally unobservable. Clark and Duane (1923, 1924) studied Compton scattering from bound electrons and argued that their observed photon energy loss values corresponded to some sort of secondary radiation emitted by photoelectrons. This work was criticised by Compton (1924).

Raman (1928) independently noted the possibility of such a happening in inelastic x-ray scattering and his colleague Krishnan (1928) was the first to observe it experimentally. Krishnan's experiments involved the scattering of MoK_α radiation from graphite. He observed that new narrow x-ray lines shifted downwards in frequency from the Rayleigh peak by about the ionization energy of the K and L electrons. The linewidths of these lines were close to the width of the exciting spectral lines, namely the MoK_α lines. Their positions were independent of the scattering angle θ in the range of 90° to 160°. Krishnan's experiments were repeated by Mitchell and Davies (1928) on graphite, Davies and Mitchell (1929) on aluminium, beryllium and graphite, Coster *et al* (1929) on beryllium and graphite and DuMond (1929) on beryllium with essentially similar results. However, the following workers failed to get experimental results similar to those obtained by Krishnan and others: Ehrenberg (1929), Kast (1929), Coster (1929), Bearden (1930) and Gingrich (1930). It is interesting to mention here that Mitchell (1929) and Davies and Purks (1929) reported to have observed anti-Stoke's lines in x-ray Raman scattering which probably were high energy satellite lines and were wrongly interpreted in terms of the Raman process. This conflicting evidence led Compton and Allison (1935) to remark in their famous book: "The existence of such (Raman) radiation as a part of scattered x-rays, though frequently suspected, has never been established. It is probably too weak to be detected".

3. Early theoretical developments

The earliest theoretical work in this area was carried out by Jauncey (1924, 1925) and this work was of a semiempirical character. Jauncey explicitly considered the motion of an electron in a Böhr orbit and applied classical radiation scattering theory to arrive at both modified and unmodified lines in the scattered radiation. Jauncey also arrived at certain conclusions from his semiclassical calculations which were years ahead of his time. The two main points made by him are: (i) a recognition that the width of the modified line, or rather the intensity distribution in the scattered spectrum yields information about the velocities of the scattering electrons, and (ii) a realization that the scattering act may correspond to different physical processes *viz* Rayleigh-Thomson, Compton or Raman; the last one was recognised but not made explicit. He calculated the relative strengths of the different processes and showed that the Raman type of scattering should occur when

$$\hbar\omega \gg E, \tag{1}$$

and

$$\frac{4\pi a}{\lambda}\sin\theta/2 \approx ka \lesssim 1, \tag{2}$$

where $\hbar\omega$ is the energy of the primary photon with wavelength λ, E is the binding energy of the scattering electron and $\hbar k$ is the magnitude of the momentum transferred in the act of scattering.

Jauncey's work was repeated using a more elaborate quantum mechanical treatment by Wentzel (1927, 1929) and later by Bloch (1934). These workers failed to note x-ray Raman scattering because they considered the incident photon to be of sufficiently high energy so that at the usual laboratory scattering angles equation (2) was not satisfied. Wentzel and Bloch predicted a shift of the Compton modified line by an amount equal to the binding energy of the scattering electron. This shift, termed as the Compton defect, was observed by Ross and Kirkpatric (1934). DuMond (1933) developed Jauncey's ideas on the width of the modified line in terms of Doppler broadening. This work brought out a whole new field of electron momentum distribution studies in solids, making the Compton scattering technique an important tool in the study of electron states in solids. However, not much attention was paid to x-ray Raman scattering despite a very lucid letter written by Sommerfeld (1936) to Compton (which was later published) predicting such a process.

Sommerfeld considered the intensity distribution of the Compton modified line as a function of wavelength or energy and concluded that there must be a sharp cut-off to the Compton band at a low wavelength corresponding to the photon energy loss value equal to the binding energy of the scattering electron. Beyond this wavelength one should be able to observe a series of discrete lines due to electronic transitions to higher unoccupied atomic levels corresponding to Raman lines. Sommerfeld also pointed out the experimental evidence given by Ray (1930) and Majumdar *et al* (1931) supporting his theoretical analysis.

4. Firm evidence regarding the Raman lines in the x-ray region

The controversy regarding x-ray Raman scattering remained dormant until Dasgupta revived it in 1950's by reporting results of some very careful experiments carried out by him first in Calcutta and later abroad on the scattering of Mo and CuK_α rays by the light elements beryllium, boron and graphite. Dasgupta (1950, 1951, 1959, 1962, 1964) observed discrete lines on the long wavelength side of the Rayleigh lines at photon energy loss values corresponding to the excitation energies of the scattering atoms. A typical curve obtained by Dasgupta is shown in figure 1. In this figure the Rayleigh-Thomson line, the Compton band and the Raman lines are well resolved. The position of the Raman lines were found to be independent of the scattering angle as expected for the Raman process. Dasgupta's experiments were repeated by some other workers. Although Weiss (1965) could not confirm the appearance of the Raman lines in the scattered x-ray spectrum, Faessler and Mühle (1966), Cooper and Leak (1966) and Suzuki (1966) confirmed their existence. Further experimental work by the Japanese and the American researchers (Suzuki 1967; Hayasi *et al* 1969; Suzuki *et al* 1970; Suzuki and Hasegawa 1975; Alexandropoulos and Cohen 1969; Cohen *et al* 1973) conclusively established the Raman effect in the x-ray region.

The first theory of x-ray Raman scattering after the work of Sommerfeld (1936) was given by Mizuno and Ohmura (1967). Further theoretical work was reported by Babushkin (1971), Kuriyama and Alexandropoulos (1971) and Kuriyama (1971).

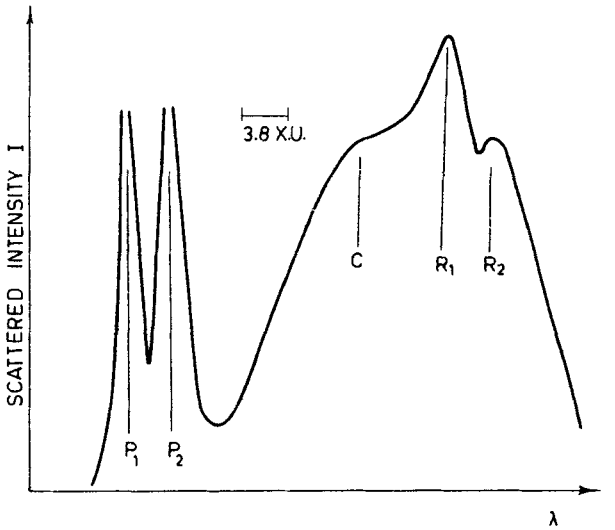

Figure 1. Raman scattering of $CuK_{\alpha_{1,2}}$ x-rays from beryllium. $\theta = 81°$, p_1 and p_2 denote the primary unmodified lines, R_1 and R_2 refer to the Raman lines and C indicates the Compton band (from Dasgupta 1962).

Actual calculations, using hydrogenic wavefunctions obtained by x-ray spectroscopy (Mande and Damle 1965; Tankhiwale and Mande 1970), of x-ray Raman scattered lineshapes were reported by Pimpale and Mande (1978). By now considerable work has been carried out on x-ray Raman scattering identifying various atomic excited states taking part in the transitions during the x-ray scattering process. Worth mentioning here are the investigations of Londos and Koumelis (1979) bringing out the possible transition of a core electron to an antibonding state in graphite and of Papadimitriou and Miliotis (1982) on polycrystalline beryllium.

The major experimental and theoretical work on x-ray Raman scattering to date is summarised in table 1 for ready reference.

5. The x-ray Raman process

The x-ray Raman process is shown schematically in figure 2. An incident photon of energy $\hbar\omega_i$ excites the system from a core state to an unoccupied discrete state, and the scattered photon comes out with energy $\hbar\omega_s$, the energy difference

$$\hbar\omega_i - \hbar\omega_s = E, \tag{3}$$

being the system excitation energy. Since the discrete states are not characterized by momentum, there is no momentum conservation equation.

Sommerfeld (1936) visualized the outer unoccupied state to be of atomic character giving rise to sharp Raman lines. In free atoms and to some extent in molecules this picture is valid but not so in a solid where one must consider bands of unoccupied levels. Thus Raman lines become Raman bands in solids, and they are also sometimes referred to as Raman edges similar to x-ray absorption edges.

Table 1. Summary of major work on x-ray Raman scattering.

Author	Brief description of work
Smekel (1923)	Theoretical prediction of x-ray Raman scattering
Raman (1928)	Independent theoretical prediction
Krishnan (1928)	First observation of x-ray Raman effect using MoK_α radiation scattered by graphite
Sommerfeld (1936)	Theoretical analysis of discrete Raman lines in Compton scattered X-radiation
Dasgupta (1950, 1951, 1959, 1962, 1964)	Careful experiments leading to observation of x-ray Raman scattering of Mo and CuK_α rays by beryllium, boron and graphite
Faessler and Mühle (1966) Cooper and Leak (1966) Suzuki (1966)	Repeated Dasgupta's experiments and confirmed the phenomenon of x-ray Raman scattering
Mizuno and Ohmura (1967)	Theory of x-ray Raman scattering
Alexandropoulos (1970, 1971)	Experimental work on x-ray Raman scattering from defects in alkali halides
Sparks (1974)	Theoretical prediction and experimental observation of internal resonance Raman scattering with Mo and CuK_α radiation scattered by Ni, Cu, Zn, Ge and Te
Eisenberger, Platzman and Winick (1976a, b)	Experimental work on internal resonance Raman scattering using a tunable synchrotron x-ray source

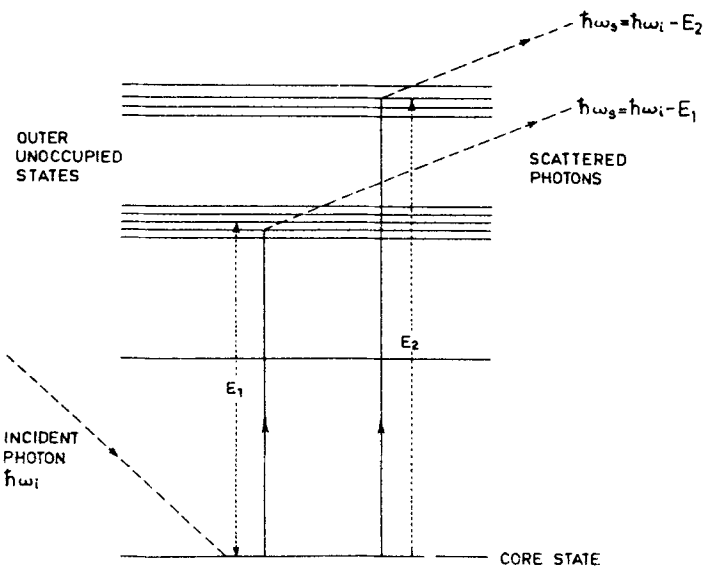

Figure 2. Schematics of x-ray Raman process.

Since the states involved in the Raman process have no well-defined momentum, it possesses the following characteristics: (i) The Raman edge does not shift with the scattering angle θ. (ii) The intensity of the scattered radiation

$$I_R \alpha (1+\cos^2\theta)\cdot\sin^2\tfrac{1}{2}\theta,$$

for excitation of an electron from the K state. The first factor is due to polarization effect and the second arises from Fourier transform of the hydrogenic wavefunction for the inner state. This latter factor will be somewhat different when one considers inner atomic levels of different symmetries. (iii) In a solid the shape of the Raman spectrum is in principle similar to the shape of the corresponding x-ray absorption edge which has generally an arc-tangent form (Richtmyer *et al* 1934). Popescu (1979) also observed extended modulation of the x-ray Raman scattering edge similar to the EXAFS (extended x-ray absorption fine structure) on the high energy side of x-ray absorption edges (Mande *et al* 1980).

It may be mentioned here that in the x-ray region one can observe only the Stoke's lines. The probability of having the system already in an excited state so that anti-Stoke's lines may be observed in an x-ray Raman process is very low, since it is not feasible to have the system in the required excited state with excitation energies of the order of a few hundred electron volts or more.

6. Theory of x-ray Raman scattering

A schematic diagram of the general act of scattering in which an incident x-ray photon of wavevector $\mathbf{k}_i$, frequency ω_i and polarization η_i interacts with a system initially in state I is shown in figure 3. The scattered photon is characterized by the subscript s and the system makes a transition to the state F. The different inelastic scattering processes envisaged by considering the nature of system states I and F are shown in table 2. In simple situations the energy and wavevector transferred by the photon in the act of scattering can be ascribed to elementary excitations of the scatterer. The dispersion relations for the relevant excitations are also given in table 2. The cross-sections of some of these processes have been discussed by us earlier (Pimpale and Mande 1975). In the following sections we present our work on a generalized theory of x-ray Raman scattering from an atomic system.

6.1 *Mathematical formulation*

Consider an atomic system with a nuclear charge Ze and mass M at $\mathbf{R}$ and N electrons (each of mass m, charge $-e$) at $\mathbf{r}_i$ ($i = 1, 2, \ldots, N$). The Hamiltonian of the system is

$$H_0 = p^2/2M + \sum_{i=1}^{N} (p_i^2/2m - Ze^2/|\mathbf{R}-\mathbf{r}_i|) + \sum_{i<j} e^2/|\mathbf{r}_i - \mathbf{r}_j|, \tag{4}$$

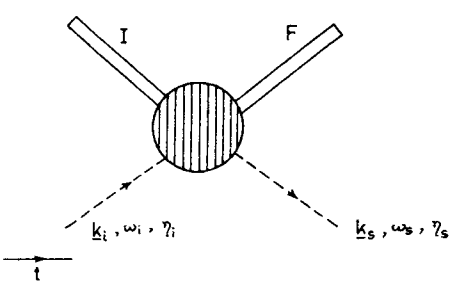

Figure 3. A general act of scattering. See text for description.

Table 2. Different x-ray inelastic scattering processes.

Scattering process	Initial state	Final state	Dispersion relation for the participating elementary excitation
Compton	Free single electron at rest	Free particle state	$\omega = \hbar k^2/2m$
Plasmon	Valence electron plasma in ground state	Plasmon	$\omega = \omega_p + ak^2$
Raman (Sommerfeld lines)	Bound single electron	(Unoccupied) Discrete single particle orbitals	$\omega = (E_F - E_I)/\hbar$
Raman band	Bound single electron	Unoccupied band states	$\omega = [E_F(\mathbf{k}) - E_I]/\hbar$
Compton scattering bound electrons	Bound single electron	Free outgoing particle in state k	$\omega = \omega_i - \lvert E_I \rvert/\hbar + \hbar k^2/2m$
*Compton-plasmon	Valence electron plasma in ground state	Plasmon + an outgoing electron in state k	$\omega = \omega_p + \frac{\hbar}{2m}\left[(\mathbf{k}+\mathbf{q})^2 - q^2\right]$

$\hbar k$: momentum transferred in the act of scattering
*see Pimpale and Mande (1971, 1974) for details
$\mathbf{q}$: Initial wavevector of scattering electron
$\omega_p = (4\pi ne^2/m)^{\frac{1}{2}}$ is the plasma frequency for the jellium with electron density n
$E_J = (J = I, F)$ are energies of electron states k.
$\hbar\omega_i$: energy of the incident photon

where $\mathbf{P}$ and $\mathbf{p}_i$ are momentum operators for the nucleus and the ith electron. Let us introduce coordinates $\mathbf{X}_0$ and $\mathbf{x}_i$ for the centre of mass of the system and the relative motion of the ith electron with respect to the nucleus through

$$M\mathbf{R} + \sum_{i=1}^{N} m\mathbf{r}_i = (M + Nm)\mathbf{X}_0, \tag{5}$$

$$\mathbf{R} - \mathbf{r}_i = \mathbf{x}_i (i = 1, 2, \ldots, N). \tag{6}$$

The Hamiltonian (4) in terms of these coordinates becomes

$$H_0 = \mathbf{p}^2_{\mathbf{x}_0}/2(M + Nm) + \sum_{i=1}^{N} (\mathbf{p}^2_{\mathbf{x}_i}/2\mu - Ze^2/x_i)$$

$$+ \sum_{i<j} (e^2/|\mathbf{x}_i - \mathbf{x}_j| + \mathbf{p}_{\mathbf{x}_i} \cdot \mathbf{p}_{\mathbf{x}_j}/M), \tag{7}$$

where $\mathbf{P}_{\mathbf{X}_0}$, $\mathbf{p}_{\mathbf{x}_i}$ are momentum operators for centre of mass motion and the relative motion of ith electron:

$$\mathbf{P}_{\mathbf{X}_0} \equiv -i\hbar\nabla\mathbf{X}_0,$$

$$\mathbf{p}_{\mathbf{x}_i} = -i\hbar\nabla\mathbf{x}_i. \tag{9}$$

μ is the usual reduced mass

$$1/\mu = 1/m + 1/M. \tag{10}$$

The first term in (7) represents the free centre of mass motion. The second term gives rise to single-electron states which are perturbed by the third and the fourth terms. The third term is the well-known electron-electron interaction. However, the fourth term is a new type of interaction arising out of dynamic coupling between electrons through the nuclear mass M. The effects of this term on electronic states of the system are analyzed elsewhere.

The interaction of the radiation with the atomic system is introduced as usual by representing the radiation vector potential $\mathbf{A}(\mathbf{r}, t)$, working in Coulomb gauge and making the transformation

$$\mathbf{P}_\mathbf{r} \rightarrow \mathbf{p}_\mathbf{r} - q\,\mathbf{A}(\mathbf{r}, t)/c, \tag{11}$$

where $\mathbf{p}_\mathbf{r}$ is the momentum operator of a particle of charge q at position $\mathbf{r}$ and c is the speed of light (see *e.g.* Adams and Landsberg 1969, Pimpale 1973 for details). By Fourier expanding the vector potential and using the centre of mass and relative coordinates the first- and the second-order interaction terms are given by

$$H_1 \equiv H_{\text{int}}(\mathbf{p}\cdot\mathbf{A}) = (4\pi e^2/V)^{\frac{1}{2}} \sum_{\mathbf{k},\mu} Q_{\mathbf{k}\mu}\eta_{\mathbf{k}\mu}\cdot \exp(i\mathbf{k}\cdot[\mathbf{X}_0 + a\mathbf{X}])\left\{(-bZ/M + \frac{a}{m}\sum_i \exp(-i\mathbf{k}\cdot\mathbf{x}_i)\mathbf{P}_{\mathbf{X}_0} - \sum_i \frac{Z}{M} + \frac{1}{m}\exp(-i\mathbf{k}\cdot\mathbf{x}_i)\mathbf{p}_{\mathbf{x}_i}\right\} \tag{12}$$

$$H_2 \equiv H_{\text{int}}(A^2) = \frac{2\pi e^2}{V} \sum_{\mathbf{k},\mathbf{k}',\mu,\mu'} Q_{\mathbf{k}\mu} Q^*_{\mathbf{k}'\mu'} \eta_{\mathbf{k}\mu}\cdot\eta_{\mathbf{k}'\mu'} \times \exp[i(\mathbf{k}-\mathbf{k}')\cdot(\mathbf{X}_0 + \mathbf{a}\mathbf{X})]\left\{\frac{Z^2}{M} + \frac{1}{m}\sum_i \exp[-i(\mathbf{k}-\mathbf{k}')\cdot\mathbf{x}_i]\right\}, \tag{13}$$

where

$$a \equiv m/(M + Nm) \ll 1, \tag{14}$$

$$b \equiv M/(M + Nm) \approx 1, \tag{15}$$

$$\mathbf{x} \equiv \sum_i \mathbf{x}_i, \tag{16}$$

V is the volume enclosing the system, $Q_{\mathbf{k}\mu}$ is the $\mathbf{k}$th Fourier component of the radiation field, $\eta_{\mathbf{k}\mu}$ is the polarization vector and μ lables the two transverse polarization modes:

$$\mathbf{k}\cdot\eta_{\mathbf{k}\mu} = 0, \qquad \mu = 1, 2. \tag{17}$$

Introducing photon creation and annihilation operators $A^+_{\mathbf{k}\mu}$, $A_{\mathbf{k}\mu}$ we get

$$H_1 = \left[\frac{4\pi e^2}{V}\right]^{\frac{1}{2}} \sum_{\mathbf{k},\mu} (\hbar/2\omega_\mathbf{k})^{\frac{1}{2}}(A_{\mathbf{k}\mu} + A^+_{-\mathbf{k}\mu})\eta_{\mathbf{k}\mu}\cdot\exp[i\mathbf{k}\cdot(\mathbf{X}_0 + a\mathbf{X})] \left(\left\{-\frac{bZ}{M} + \frac{a}{m}\sum_i \exp(-i\mathbf{k}\cdot\mathbf{x}_i)\right\}\mathbf{P}_{\mathbf{X}_0} - \sum_i\left[\frac{Z}{M} + \frac{1}{m}\exp(-i\mathbf{k}\cdot\mathbf{x}_i)\right]\mathbf{P}_{\mathbf{x}_i}\right) \tag{18}$$

$$H_2 = \frac{2\pi e^2}{V} \sum_{\mathbf{k},\mu,\mathbf{k}',\mu'} (\hbar^2/4\omega_{\mathbf{k}}\omega_{\mathbf{k}'})^{\frac{1}{2}} (A_{\mathbf{k}\mu} + A^{+}_{-\mathbf{k}\mu})\,(A^{+}_{\mathbf{k}'\mu'} + A_{-\mathbf{k}'\mu'})$$
$$\eta_{\mathbf{k}\mu}\cdot\eta_{\mathbf{k}'\mu'} \exp[i(\mathbf{k}-\mathbf{k}')\cdot(\mathbf{X}_0 + a\mathbf{X})]$$
$$\{Z^2/M + 1/m \sum_i \exp[-i(\mathbf{k}-\mathbf{k}')\cdot\mathbf{x}_i]\}. \tag{19}$$

In first order of perturbation H_1 contributes to single-photon processes (emission or absorption of a light quantum) and H_2 contributes to two-photon processes (emission or absorption of two light quanta or emission of one light quantum and absorption of another light quantum). It may be remarked that in the limit

$$a \to 0,\ b \to 1, \tag{20}$$

the coupling between the electron and nuclear motions brought about through radiation interaction as seen in (18) and (19) is broken. The details of the new aspects of electromagnetic interactions brought about through such a coupling will be discussed elsewhere. In the above formulation explicit coupling of the radiation magnetic field with the electronic and nuclear spins is ignored. This is usually justifiable for x-ray scattering as shown, for example, by Eisenberger and Platzman (1970), Platzman and Tzoar (1970).

6.2 *Matrix element for scattering*

Consider the scattering act shown in figure 3. The matrix element $M(A^2)$ from the A^2-term (13) is obtained from (19) as

$$M(A^2) = \frac{4\pi e^2}{V} (\hbar^2/4\omega_i\omega_s)^{\frac{1}{2}} [n_i(n_s+1)]^{\frac{1}{2}} \eta_i\cdot\eta_s\, \delta\mathbf{K}_S - \mathbf{K}_I,\, \mathbf{q}$$
$$\left\{\frac{Z^2}{M}\int d^3\mathbf{x}_1 \ldots \int d^3\mathbf{x}_N \phi^{S^*}_{\mathrm{Rel}} \exp(ia\mathbf{q}\cdot\mathbf{x})\phi^{I}_{\mathrm{Rel}}\right.$$
$$\left. + \frac{1}{m}\int d^3\mathbf{x}_1 \ldots \int d^3\mathbf{x}_N \phi^{S^*}_{\mathrm{Rel}} \exp[i\mathbf{q}\cdot(a\mathbf{x}-\mathbf{x}_i)]\phi^{I}_{\mathrm{Rel}}\right\} \tag{21}$$

with

$$\mathbf{q} = \mathbf{k}_s - \mathbf{k}_i.$$

In (21) the system wavefunction is taken as

$$\phi^{\alpha}_{CM}(\mathbf{X}_0)\phi^{\alpha}_{\mathrm{Rel}}(\mathbf{x}_1, \ldots, \mathbf{x}_N) = \frac{1}{\sqrt{V}} \exp(i\mathbf{k}_\alpha\cdot\mathbf{X}_0)\phi^{\alpha}_{\mathrm{Rel}}, \quad \alpha = I, S \tag{22}$$

The process corresponding to (21) is shown in figure 4.

The $\mathbf{p}\cdot\mathbf{A}$-term (12) or (18) gives rise to two scattering processes as shown in figure 5 and the corresponding matrix elements are:

Process (a)

$$M(\mathbf{p}\cdot\mathbf{A}) = \sum_J \frac{4\pi e^2}{V} (\hbar^2/4\omega_i\omega_s)^{\frac{1}{2}} [n_i(n_s+1)]^{\frac{1}{2}}$$
$$\frac{\langle S|G(-\mathbf{k}_s, \mu_s)|J\rangle\langle J|G(\mathbf{k}_i, \mu_i)|I\rangle}{E_I - E_J + \hbar\omega_i} \tag{23}$$

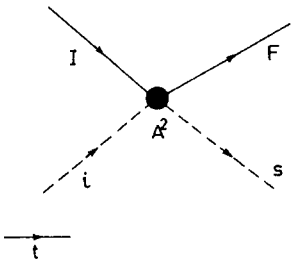

Figure 4. Scattering process due to the A^2-term in the interaction Hamiltonian.

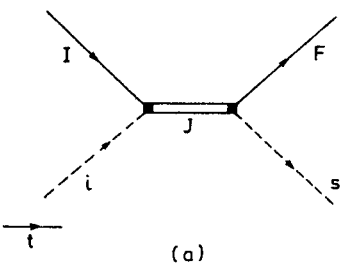

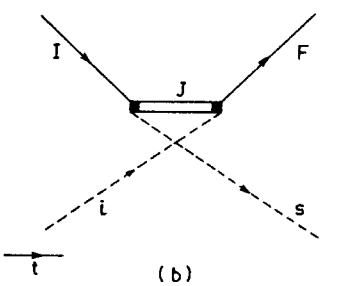

Figure 5. Scattering processes due to the $\mathbf{p}\cdot\mathbf{A}$-term in the interaction Hamiltonian.

Process (b)

$$M(\mathbf{p}\cdot\mathbf{A}) = \sum_J \frac{4\pi e^2}{V}(\hbar^2/4\omega_i\omega_s)^{\frac{1}{2}}[n_i(n_s+1)]^{\frac{1}{2}} \frac{\langle S|G(\mathbf{k}_i,\mu_i)|J\rangle\langle J|G(-\mathbf{k}_s,\mu_s)|I\rangle}{E_I - E_J - \hbar\omega_s}, \tag{24}$$

where

$$G(\mathbf{k},\mu) = \eta\cdot\exp[i\mathbf{k}\cdot(\mathbf{X}_0 + a\mathbf{X})]\left(\left\{-bZ/M + \frac{a}{m}\exp(-i\mathbf{k}\cdot\mathbf{x}_i)\right\}\mathbf{P}_{\mathbf{X}_0} - \sum_i\left\{Z/M + \frac{1}{m}\exp(-i\mathbf{k}\cdot\mathbf{x}_i)\right\}\mathbf{p}_{\mathbf{x}_i}\right). \tag{25}$$

In (23), (24) and (25) J represents various intermediate states. When

$$\hbar\omega_i \approx \hbar\omega_s \gg |E_I - E_J|, \tag{26}$$

the contributions to scattering from (21) and (24) are negligible as compared with that from (21) due to large energy denominators. In many situations pertaining to x-ray Raman scattering (26) is satisfied and the A^2-term in the Hamiltonian gives the dominant contribution. This is true for other scattering acts in the x-ray region as well (see *e.g.* Heitler 1954; Ohmura and Matsudiara 1964).

The differential scattering cross-section per unit frequency per unit solid angle is obtained from the matrix element M as

$$\frac{d^2\sigma}{d\omega\, d\Omega} = \sum \frac{\omega_i}{\omega_s}\left[\frac{V}{2\pi}\right]^2 \frac{\omega_s^2}{c^4 n_i \hbar} |M|^2 \delta \text{ (energy conservation)}.$$

where the summation is over all available final electron states. (27)

6.3 *Single-particle approximation*

We now make single-particle approximation for the wavefunction $\phi^{\alpha}_{\text{Rel}}$ in (22) representing the relative motion of N electrons with respect to the nucleus. Let $\chi^{\alpha}_f(\mathbf{x}_i)$ be the wavefunction for ith electron in state f when the total system state is designated by α. Then, taking determinantal wavefunction

$$\phi^{\alpha}_{\text{Rel}} = \frac{1}{(N!)^{\frac{1}{2}}} \sum_{i,j,\ldots,z=1}^{N} \varepsilon_{ij\ldots z}\chi^{\alpha}_i(\mathbf{x}_1)\chi^{\alpha}_j(\mathbf{x}_2)\ldots\chi^{\alpha}_z(\mathbf{x}_N),$$

$$\alpha = I, S \tag{28}$$

where $\varepsilon_{ij\ldots z}$ is a completely antisymmetric tensor of rank N. Assuming that in making a transition from electronic state ϕ^{I}_{Rel} to ϕ^{S}_{Rel} in the act of scattering only one single-particle state is changed, say χ_I becomes χ_S, the first integral in (21) becomes, for $a \ll 1$

$$\int d^3\mathbf{x}_1 \ldots \int d^3\mathbf{x}_N\, \phi^{S^*}_{\text{Rel}} \exp(ia\mathbf{q}\cdot\mathbf{x})\phi^{I}_{\text{Rel}}$$

$$\approx ia\mathbf{q}\cdot\int d^3\mathbf{y}\,\chi^*_S(\mathbf{y})\mathbf{y}\,\chi_I(\mathbf{y}). \tag{29}$$

The contribution of second integral in (21) is approximately $(Z/4000)^{-1}$ times that due to the first term owing to the Z^2/M factor. When the approximation $a \to 0$ is made the coupling between the nuclear and the electronic motions is lost. The second term in curly bracket in (21) then gives a contribution

$$\int d^3\mathbf{y}\,\chi^*_S(\mathbf{y})\exp(-i\mathbf{q}\cdot\mathbf{y})\chi_I(\mathbf{y}). \tag{30}$$

6.4 *Raman cross-section*

Consider the Raman process in which the final single-particle state is a plane wave state of momentum $\hbar\mathbf{p}$ and energy $\hbar^2p^2/2m$ and assume the initial state to be a K level

described by a hydrogenic wavefunction. The matrix element is then obtained from (21) and (30) as

$$M = \frac{C}{m}\cdot\frac{8}{\pi}\cdot(8\pi^3/V)^{\frac{1}{2}}\,(Z_K/a_0)^{5/2}\,(Z_K^2/a_0^2+|\mathbf{p}-\mathbf{q}|^2)^{-2}, \tag{31}$$

where a_0 is the Böhr radius, Z_K is the effective nuclear charge and the constant C is defined by

$$C = (4\pi e^2/V)\cdot(\hbar^2/4\omega_i\omega_s)^{\frac{1}{2}}\cdot[n_i(n_s+1)]^{\frac{1}{2}}\eta_i\cdot\eta_s. \tag{32}$$

From (27), (31) and (32) the differential scattering cross-section is given by

$$\begin{aligned}\frac{d^2\sigma}{d\omega d\Omega} = {} & \frac{2^8(\hbar/mc)^3}{3\pi c Z_K^2}\cdot(1+\cos^2\theta)\cdot(\omega_s^2/\omega_i^2)\cdot(pa_0/Z_K)\\ & \times\{3(1+[p^2+q^2]a_0^2/Z_K^2)^2-4p^2q^2a_0^4/Z_K^4\}.\\ & \times\{(1+[p^2+q^2]a_0^2/Z_K^2)^2-4p^2q^2a_0^4/Z_K^4\}^{-3},\end{aligned} \tag{33}$$

where

$$p^2a_0^2 = (2\hbar\omega_i/mc^2)\,(\hbar c/e^2)^2\,(1-[\hbar\omega_s+E_K]/\hbar\omega_i), \tag{34}$$

$$q^2a_0^2 = (\hbar\omega_i/mc^2)\,(\hbar c/e^2)^2(1-\omega_s\cos\theta/\omega_i+\omega_s^2/\omega_i^2). \tag{35}$$

In (33) photon polarization effects have been averaged out and θ is the scattering angle. The Raman cross-section $d\sigma/d\Omega$ is compared with typical Compton and plasmon cross-sections in table 3.

7. Discussion of some experimental results

In most experiments the x-ray source is a sealed x-ray tube operated at about 40 to 50 kV and 50 to 100 mA. A typical experimental arrangement is shown schematically in figure 6. Experimental Raman spectra for lithium, beryllium, boron and graphite for different scattering angles are shown in figure 7. Shapes of the Raman bands are obtained from the experimental spectra by unfolding them. The unfolded Raman band

Table 3. Numerical comparison of cross-sections of different x-ray scattering processes for the case of CrK_β radiation incident on beryllium. Scattering angle $\theta = 40^\circ$

Scattering process	Cross-section $d\sigma/d\Omega$ (cm^2)
Rayleigh-Thomson	$4{\cdot}65\times10^{-26}$
Compton (RPA)	$3{\cdot}95\times10^{-27}$
Raman	$4{\cdot}00\times10^{-28}$
*Plasmon	$2{\cdot}65\times10^{-26}$
*Compton-plasmon	$2{\cdot}6\times10^{-27}$

* For this scattering angle $k \sim 2{\cdot}06\,\text{Å}^{-1} > k_c$, the plasmon cut-off wavevector and the plasmon band becomes very broad.

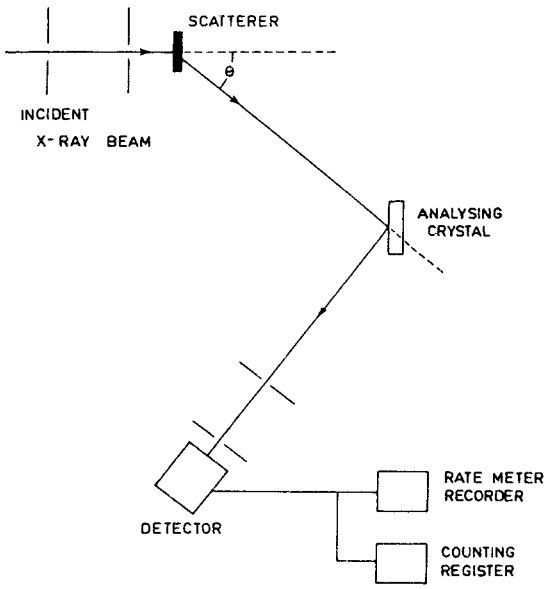

Figure 6. Schematics of an x-ray scattering experiment.

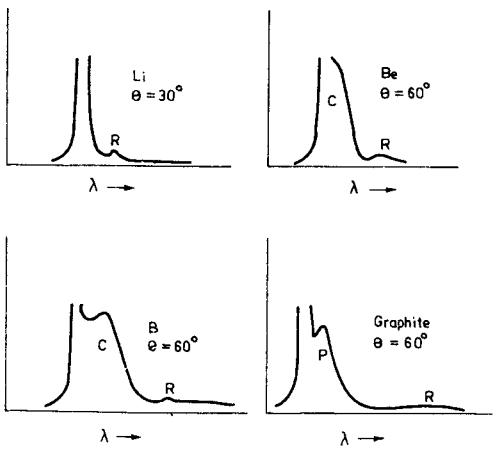

Figure 7. Some experimental Raman spectra for lithium, beryllium, boron and graphite using incident CrK_α radiation (from Suzuki *et al* 1970).

for a typical case is shown in figure 8. The calculated Raman spectrum is also shown in this figure after matching the peak positions with the experimental values. The second hump in the experimental curve is seen to be not present in the calculated curve. Probably it represents band structure effects which were not incorporated in our calculations (see *e.g.* Papadimitriou and Miliotis 1982).

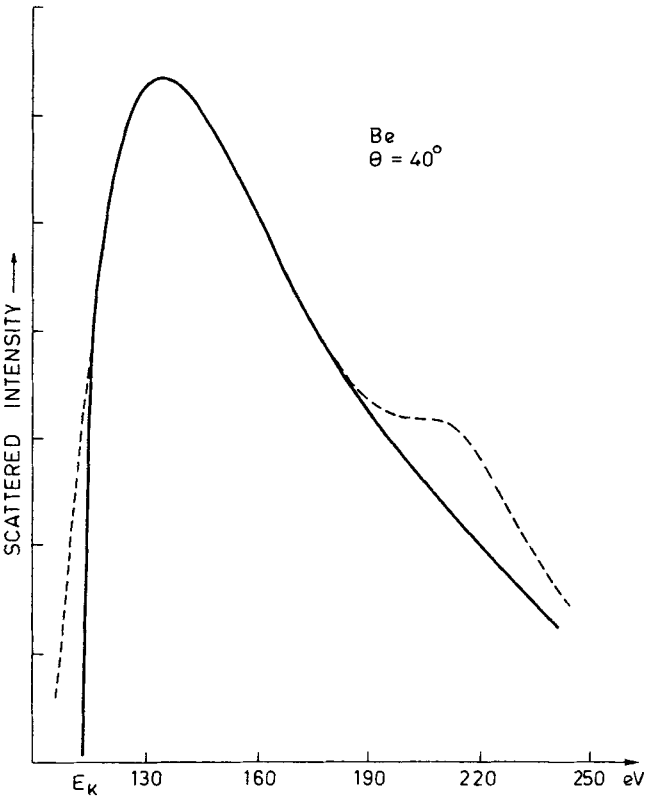

Figure 8. Unfolded experimental and calculated Raman spectra for beryllium ($\theta = 40°$).

8. Internal resonance Raman scattering

When condition (1) is not valid one must consider the second-order contributions from the $\mathbf{p}\cdot\mathbf{A}$ term in the interaction Hamiltonian. The corresponding matrix element (23) becomes very large when the energy denominator in it becomes very small, *i.e.* in situations when the excited states J satisfy

$$E_J = E_I + \hbar\omega_i. \tag{36}$$

When (36) is satisfied there is a resonance process and the Raman cross-section increases substantially. The resonance process may be described as shown in figure 9. The incoming photon of energy $\hbar\omega_i$ is absorbed by (say) a K-shell electron leading to an intermediate state E_J with a K-shell hole. This hole is filled by (say) an L-shell electron emitting the out going photon with energy $\hbar\omega_s$:

$$\hbar\omega_s = \hbar\omega_i - E_\alpha. \tag{37}$$

The final state thus contains an L-shell hole.

The possibility of such a resonance process due to the $\mathbf{p}\cdot\mathbf{A}$ term in the interaction Hamiltonian was first realized by Sparks (1974) who also observed it experimentally using CuK_α and MoK_α radiation scattered by Ni, Cu, Zn, Ge and Te at a scattering angle of about 70°. For $E_j - E_I$ close to $\hbar\omega_i$ Sparks observed a large increase in x-ray

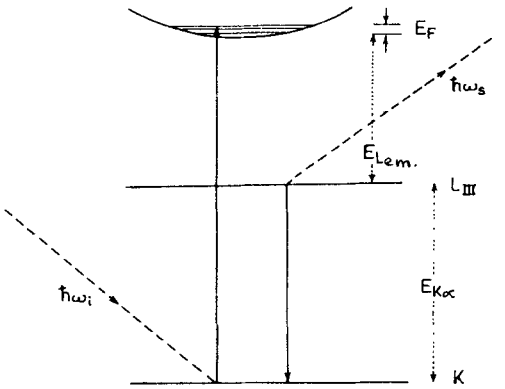

Figure 9. Schematics of internal resonance Raman scattering. Resonance occurs when $\hbar\omega_i - \hbar\omega_s = E_L + E_F$.

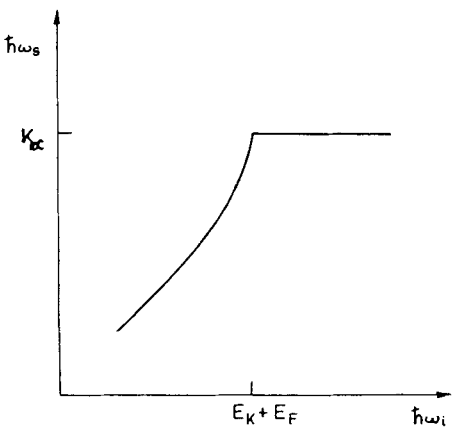

Figure 10. Variation of IRRS scattered frequency with incident frequency using a tunable synchrotron radiation source (from Eisenberger *et al* 1976b).

Raman scattered intensity and he termed the process as internal resonance Raman scattering (IRRS). The IRRS theory was given by Sparks (1974) and later elaborated by Bannett *et al* (1977), Gavrila and Tugulea (1975). Experiments of Sparks were repeated by Eisenberger and his colleagues using a tunable synchrotron x-ray source and they confirmed the IRRS. They also showed how IRRS goes over to x-ray fluorescence when the incident photon energy goes over smoothly to characteristic absorption edge energies (Eisenberger *et al* 1976a, 1976b). This is shown schematically in figure 10. Fluorescence and IRRS have also been studied experimentally by Suortti (1979) in transition metals. Kodre and Shafroth (1979) and Hall *et al* (1979) studied IRRS for K-M scattering in thick silicon targets. Experiments on IRRS have also been carried out by Briand *et al* (1981) for $KMnO_4$ using synchrotron radiation of frequency in the neighbourhood of the white line in Mn *K*-absorption spectrum.

9. Concluding remarks

In the previous sections we have shown that there exists sufficient evidence for the occurrence of Raman type of scattering in the x-ray region. We have been able to calculate, using x-ray spectroscopically obtained hydrogenic wavefunctions for the discrete core states, the cross-sections of the Raman process for some experimental situations. A comparison of the cross-sections of this process with those of other processes like Rayleigh-Thomson, Compton and plasmon scatterings shows that the probability of observing Raman scattering in the x-ray region is not quite negligible. With the advent of new powerful x-ray sources like the synchrotron storage rings and the development of spectrographs of higher resolving power, it may now be possible to carry out more meaningful experiments on the scattering phenomena in the x-ray region. The study of Raman lines or bands in the x-ray region will, it is hoped, provide fruitful information regarding the outer electron states of atoms, molecules and solids, complementary to that presently available from x-ray absorption and photoelectron spectroscopic work.

Acknowledgement

The authors would like to thank Professor A S Nigavekar for cooperation.

References

Adams M J and Landsberg P T 1969 *Gallium arsenide lasers* (ed.) C H Gooch (London: Wiley)
Alexandropoulos N G and Cohen G G 1969 *Phys. Rev.* **187** 455
Alexandropoulos N G 1970 *Phys. Rev.* **B1** 4115
Alexandropoulos N G 1971 *Phys. Rev.* **B3** 2670
Babushkin I A 1971 *Acta Phys. Pol.* **A40** 183
Bannett Y B, Rapaport D C and Freund I 1977 *Phys. Rev.* **A16** 2011
Bearden J A 1930 *Phys. Rev.* **35** 1427
Bearden J A 1930a *Phys. Rev.* **36** 791
Bloch F 1934 *Phys. Rev.* **46** 674
Briand J P, Girard D, Kostroun V D, Chevalier P, Wohrer K and Mosse J P 1981 *Phys. Rev. Lett.* **46** 1625
Bushnev V A and Kuz'min R N 1977 *Sov. Phys. Usp.* **20** 406
Clark G L and Duane W 1923 *Proc. Natl. Acad. Sci.* **9** 412, 419
Clark G L and Duane W 1924 *Proc. Natl. Acad. Sci.* **10** 41
Cohen G G, Alexandropoulos N G and Kuriyama M 1973 *Phys. Rev.* **B8** 5427
Compton A H 1923 *Phys. Rev.* **22** 409
Compton A H 1924 *Phys. Rev.* **24** 168
Compton A H and Allison S K 1935 X-rays in theory and experiment (New Delhi: Affiliated East-West Press) p. 239
Cooper M and Leah J A 1966 *Philos. Mag.* **13** 603
Coster D 1929 *Nature (London)* **123** 642
Coster D, Nitta I and Thijssen W J 1929 *Nature (London)* **124** 1230
Dasgupta K 1950 *Nature (London)* **166** 536
Dasgupta K 1951 *Nature (London)* **167** 313
Dasgupta K 1959 *Phys. Rev. Lett.* **3** 38
Dasgupta K 1962 *Phys. Rev.* **128** 2181
Dasgupta K 1964 *Phys. Rev. Lett.* **13** 338
Davies B and Mitchell D P 1928 *Phys. Rev.* **32** 331

Davies B and Purks D 1929 *Phys. Rev.* **34** 1
DuMond J W M 1929 *Phys. Rev.* **33** 643
DuMond J W M 1933 *Rev. Mod. Phys.* **5** 1
Ehrenberg W 1929 *Z. Phys.* **53** 234
Eisenberger P and Platzman P M 1970 *Phys. Rev.* **A2** 415
Eisenberger P, Platzman P M and Winick H 1976 *Phys. Rev. Lett.* **36** 623
Eisenberger P, Platzman P M and Winick H 1976a *Phys. Rev.* **B13** 2377
Faessler A and Muhle P 1966 *Phys. Rev. Lett.* **17** E574 1
Gavrila M and Tugulea M N 1975 *Rev. Roum. Phys.* (*Rumania*) **20** 209
Gingrich N S 1930 *Phys. Rev.* **35** 1444
Gingrich N S 1930a *Phys. Rev.* **36** 1050
Hall J M, Jamison K A, Weaver O L and Richard P 1979 *Phys. Rev.* **A19** 568
Hayasi T, Suzuki M and Hayasi Y 1969 *Sci. Rep. Tohoku Univ.* Ser. I Vol. 52 No. 1
Heitler W 1954 *The quantum theory of radiation*, 3rd edn (London: Oxford University Press)
Jauncey G E M 1924 *Phys. Rev.* **24** 204
Jauncey G E M 1925 *Phys. Rev.* **25** 723
Kast W 1929 *Z. Phys.* **58** 510
Kodre A F and Shafroth S M 1979 *Phys. Rev.* **A19** 675
Krishnan K S 1928 *Nature* (*London*) **122** 961
Kuriyama M and Alexandropoulos N G 1971 *J. Phys. Soc. Jpn* **31** 561
Kuriyama M 1971 *Acta Crystallogr.* **A27** 634
Londos C A and Koumelis C N 1979 *Solid State Commun.* **31** 735
Majumdar R C, Bhargava S and Mukerjee J B 1931 *Nature* (*London*) **127** 92, 273
Mande, C, Apte M and Kondawar V 1981 *Trans. Indian Inst. Metals* **34** 376
Mande C and Damle P S 1966 *Proc. Phys. Soc.* **87** 1005
Mitchell D and Davies B 1928 *Phys. Rev.* **31** 1119
Mitchell D 1929 *Phys. Rev.* **33** 871
Mizuno Y and Ohmura Y 1967 *J. Phys. Soc. Jpn.* **22** 445
Ohmura Y and Matsudiara N 1964 *J. Phys. Soc. Jpn.* **19** 1355
Papadimitriou D K and Miliotis D M 1982 *J. Phys. Soc. Jpn.* **51** 2966
Pimpale A 1973 *A study of electron states in solids* Ph.D. Thesis Nagpur Univ. (unpublished)
Pimpale A and Mande C 1971 *J. Phys.* **C4** 2593
Pimpale A and Mande C 1974 *Phys. Fenn.* (*Finland*) **9** Suppl. S1 376
Pimpale A and Mande C 1975 *Indian J. Phys.* **49** 355
Pimpale A and Mande C 1975a *J. Phys.* **C8** 2463
Pimpale A and Mande C 1978 *Int. Conf. x-ray and XUV Spectr.* Sendai (Japan)
Platzman P M and Tzoar N 1965 *Phys. Rev.* **A139** 410
Platzman P M and Tzoar N 1970 *Phys. Rev.* **B2** 3556
Popescu M 1979 *Phys. Lett.* **A73** 260
Raman C V 1928 *Indian J. Phys.* **2** 387
Ray B B 1930 *Z. Phys.* **66** 261
Richtmyer F K, Barnes S W and Ramberg E 1934 *Phys. Rev.* **46** 843
Ross P A and Kirkpatric P 1934 *Phys. Rev.* **46** 668
Schulke W and Berg U 1967 *Phys. Status Solidi* **23** K87
Smekel A 1923 *Naturwissenschaften* **11** 873
Sommerfeld A 1936 *Phys. Rev.* **50** 38
Sparks Jr C J 1974 *Phys' Rev. Lett.* **33** 262
Suortti P 1979 *Phys. Status Solidi* **B91** 657
Suzuki T 1966 *J. Phys. Soc. Jpn.* **21** 2087
Suzuki T 1967 *J. Phys. Soc. Jpn.* **22** 1139
Suzuki T, Kishimoto T, Kaji T and Suzuki T 1970 *J. Phys. Soc. Jpn.* **29** 730
Suzuki T and Nagasawa H 1975 *J. Phys. Soc. Jpn.* **39** 1579
Tankhiwale A V and Mande C 1970 *J. Phys.* **B3** 774
Weiss R J 1965 *Phys. Rev.* **140** A1867
Wentzel G 1927 *Z. Phys.* **43** 1, 779
Wentzel G 1929 *Z. Phys.* **58** 348